CHARACTERIZATION AND EVALUATION OF POLYMER THIN FILM COMPOSITES FROM RICE STRAW MICROCRYSTALLINE CELLULOSE AND MUSHROOM CHITOSAN

Sam Sung Ting[1,2*], Madah Hussain[1], Noorulnajwa Diyana Yaacob[1], Nur Mawaddah Majib[1], Siti Nurain Hamimi[1], Tan Lian See[3] and Tan Wai Kian[4]

[1]Faculty of Chemical Engineering & Technology, Universiti Malaysia Perlis (UniMAP), Arau, 02600, Perlis, Malaysia.
[2]Centre of Excellence Geopolymer and Green Technology (CEGeoGTech), Universiti Malaysia Perlis, Kompleks Pusat Pengajian Jejawi 2, Taman Muhibbah, Arau, 02600, Perlis, Malaysia.
[3]Department of Chemical Process Engineering, Malaysia-Japan International Institute of Technology, Universiti Teknologi Malaysia, 54100 Kuala Lumpur, Malaysia
[4]Institute of Liberal Arts and Sciences, Toyohashi University of Technology, Toyohashi 441-8580, Aichi, Japan.

*stsam@unimap.edu.my

Abstract. The composite thin films functionally provide appropriate mechanical properties for specific purposes in the packaging industry. The composite film could be prepared by mixing rice straw extracted microcrystalline cellulose (MCC) with mushroom chitosan (MCH). The advantage of using mushroom chitosan is that the material is free of allergic sources from animals. In this study, *Boletus edulis* (porcini mushroom) was chosen as the raw material for the extraction of chitin and was converted to chitosan. The MCH/MCC biocomposites film was prepared by using solution casting method. The performance of the composites was evaluated using tensile test, scanning electron microscopy (SEM) and X-Ray diffraction analysis (XRD). For tensile test, MCH/MCC biocomposites with 8% MCC demonstrated an optimum tensile strength, elongation at break and Young's modulus. The tensile strength and elongation at break reduced at 10% MCC content. SEM micrograph showed lesser pores on the surface of MCC/MCH biocomposites with 8% MCC as compared to 10% MCC content. According to XRD results, the addition of MCC into MCH has increased the crystallinity of the MCH/MCC composites. This research presents a novel combination of mushroom-based chitosan (MCH) and microcrystalline cellulose (MCC) to form composite thin films, offering a sustainable and allergen-free alternative with enhanced mechanical properties suitable for a wide range of potential applications like the packaging industry.

Keywords: mushroom chitosan, composite film, microcrystalline cellulose, rice straw

Article Info

Received 9th January 2024
Accepted 9th June 2024
Published 12th June 2024

ISSN: 1823-7010, eISSN: 2600-7444

1. INTRODUCTION

Over the last few years, interest in research and development of edible films has increased. These films are gaining much popularity, and they are primarily composed of proteins such as soy protein, wheat protein, and kidney bean protein, as well as polysaccharides like starch, cellulose, and chitosan, along with lipids[1-3].When compared to synthetic packaging materials typically employed in the chemical industry, biopolymer-based films hold the potential to substitute petroleum-based plastic packaging films, thereby mitigating their environmental footprint[4]. Polysaccharide based edible films exhibit chemical stability and can be customized for extended periods of storage in diverse environmental conditions which maintaining excellent physical and mechanical qualities[1].

Chitin and Chitosan, due to their numerous favorable qualities, have attracted the attention of the industry men and the scientists' equally. These two biomolecules have wide applications in the biomedicine, paper making, food industry, and agriculture and textile industry [5].Various qualities of chitin and chitosan including non-toxicity and biodegradability make their applicability in these areas [6]. It has some unique features such as sorption, antimicrobial, film-forming, and wound healing. These unusual qualities of this substance have attracted the attention of scientists. Chitosan extraction from crustacean shells faces challenges with seasonal raw materials availability, high chemical usage, and high energy consumption[7]. Therefore, the use of fungi as source for chitin nanofiber production offers a notable advantage due to the simpler and lower-energy defibrillation processes involved. *Boletus edulis* and its related species are some of the most widely and frequently harvested edible mushrooms in the world [8]. Native to Europe, *Boletus edulis* is now found globally, including in China, Japan, and North America [9]. *B. edulis* is characterized by a bun-shaped brown cap, white reticulation on the upper stipe, pale yellow to olive-brown pores, aromatic white flesh, and non-staining characteristics when cut [10]. Incorporating *B. edulis* as a fungal source for chitosan production can reduce the overall cost of the extraction of chitosan and the nanofiber process. It highlights the effectiveness of the cost of utilizing fungi compared to crustaceans for chitin nanofiber production [11].However, the molecular weight of the chitosan is high due to it dissolves poorly in neutral pH solutions and has a high viscosity in aqueous solutions, ultimately it poses limitations in its usability for applications in health, food, and agriculture.

Microcrystalline cellulose (MCC), a cellulose derivative, is a well-known crystalline micrometric powder recognized for its excellent biocompatibility, biodegradability, and strong mechanical properties [12]. MCC, obtained from native cellulose, has attracted significant attention for its role in production of micro-composites. The interest arose from its remarkable ability for microscale reinforcement, characterized by a substantial presence of a large surface area for the interfacial bonding matrix and ordered crystalline regions, and noteworthy mechanical strength and stiffness, surpassing that of cellulose itself [13].MCC exhibits low permeability and the capability to create a dense percolating network through hydrogen bonds.

MCC is produced by treating cellulose with mineral acids, hydrolyzing it into small crystalline particles. These particles are subsequently refined to achieve a fine powder with a uniform particle size distribution. The resulting MCC powder is white, odorless, tasteless, and water insoluble. Certain packaging materials, especially in the food industry, utilize MCC-based films or coatings to enhance the barrier properties of the packaging [14].

In current study, the MCH/MCC biocomposite films were prepared by adding the MCC to reinforce the mushroom chitosan. All the composite films were subjected to the tensile test, Fourier Transform Infrared Spectroscopy (FTIR), X-ray diffraction analysis (XRD) and scanning electron microscopy (SEM).

2. MATERIALS AND METHODS

2.1 Materials

The rice straw was collected from paddy field in Perlis, Malaysia. The rice straw was ground and sieved with a 125 µm size. Then the ground particles were cleaned and dried at 80 °C. The matured fruiting body of *Boletus edulis* mushroom was collected from coastal area Kuala Perlis, Perlis, Malaysia. The sodium chlorite was purchased from Acros Organic (Geel, Belgium). Other chemicals includes Hydrogen peroxide, calcium chloride, sodium chloride, ethanol absolute potassium carbonate, magnesium sulphate and ammonium chloride were acquired from HmBG Chemicals (Hamburg, Germany). Glycerol, sulfuric acid, dipotassium hydrogen phosphate, potassium were obtained from Merck (Darmstadt, Germany).

2.2 Mushroom Chitosan Preparation

The fruiting body of *Boletus edulis* mushroom was washed several times, blotted dried, lyophilized and ground into fine powder using a blender. The powder was kept at the temperature of -20 °C until further use. Dried *B. edulis* was homogenized in deionized water and sonicated. Then, the suspension was centrifuged and the precipitate was subjected to deproteinization with sodium hydroxide treatment at 100 ºC for 2 hours. The deproteinization was carried out twice in order to remove the protein from chitin completely. Then, the mixture was washed using deionized water and centrifuged again. Decolorization was performed by using hydrogen peroxide solution. For the purpose of N-deacetylation, the chitin was treated with 30 wt% sodium hydroxide solution at 100 ^{O}C for 2 hours. After filtration, the chitosan was washed with deionized water until its pH reaches neutral and then freeze dried [15]. Figure 1 indicates the preparation steps of the *Boletus edulis* mushroom chitosan powder.

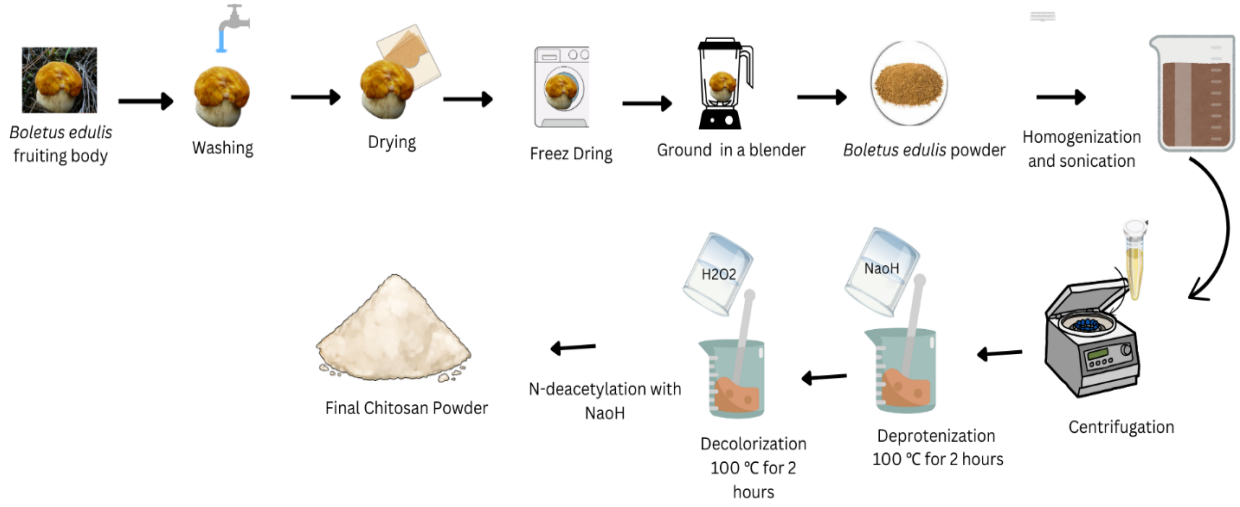

Figure 1: Schematic diagram of the preparation of *Boletus edulis* mushroom chitosan powder

2.3 Isolation of Microcrystalline Cellulose (MCC)

Two treatments were applied to rice straw which are alkaline treatment and bleaching treatment. Therefore, acid hydrolysis was used to separate the MCC from the rice straw fibre.

2.4 Alkaline Treatment

40 g of rice straw fibre (powder) was treated with an alkaline treatment by dissolving 32 g of sodium hydroxide (NaOH) (4% w/v) in 800 ml of distilled water in a 1: 20 ratio. This treatment was stirred for 2 hours at 80 °C at a rate of 350 rpm. Following that, the fibre was filtered and washed with distilled water until it reached pH [16].

2.5 Bleaching Treatment

The alkaline-treated mixture was mixed and stirred in the prepared bleaching solution. An acetic buffer, 1.7% (w/v) $NaClO_2$, and distilled water make up a bleaching solution [16]. First, an acetic buffer was made with 40 g of sodium hydroxide, 75 mL of acetic acid, and 925 mL of distilled water. The bleaching solution was prepared by combining the acetic buffer, $NaClO_2$, and distilled water in a 1:1:1 ratio, each with a volume of 267 ml. The alkaline treatment mixture was mixed with the bleaching solution and stir at 350 rpm for 2 hours at 80 °C. The treated fibre was thoroughly cleaned using distilled water. To obtain the white color form of fibre, the alkaline and bleaching treatments was cyclically repeated for two rounds. Then, the fibre was dried in the oven for 24 hours at 60 °C.

2.6 Acid Hydrolysis

The bleached fibre was subjected to acid hydrolysis in order to remove cellulose and remaining hemicelluloses and extract crystalline particles from a variety of cellulose sources. In this treatment, 2 g of cotton-like dried treated rice straw fibre was blended and add to sulfuric acid (64 wt%) at 45 °C for 1 hour at a consistent 700 rpm stirring rate. The solution was treated with 500 ml of cold distilled water to halt the reaction process. The suspension was obtained after the solution keeps at room temperature for at least 30 minutes. Most of the extracted MCC appeared to be rod-shaped fiber.

2.7 MCC/ MCH Film Preparation

About 2.25 g of mushroom chitosan powder was mixed with 150 ml of distilled water to make 1.5% (w/v) chitosan. The mixture was treated with 3 ml of 2% (v/v) acetic acid and stir for 5 hours at a rate of 700 rpm at a temperature of 60 °C. Meanwhile, 10 wt% glycerol was added to the mixture during the fourth hours of stirring to improve the flexibility of the chitosan film. Throughout the 5 hours, the beaker was wrapped in aluminium foil. In each mushroom chitosan preparation, a different content of MCC (0, 2, 4, 6, 8 and 10 wt%) was mixed with the mushroom chitosan solution. During the fourth hour of stirring the mushroom chitosan solution, MCC was added after adding the glycerol. After 5 hours, the mixture was sonicated for 10 minutes to remove any bubbles that formed. For analysis, the mixture was poured into two plastic petri dishes for repetition. In this process, the film was dried in an oven at 50 °C for 2 to 3 days with no fan. Figure 2 shows the preparation of MCC/MCH film.

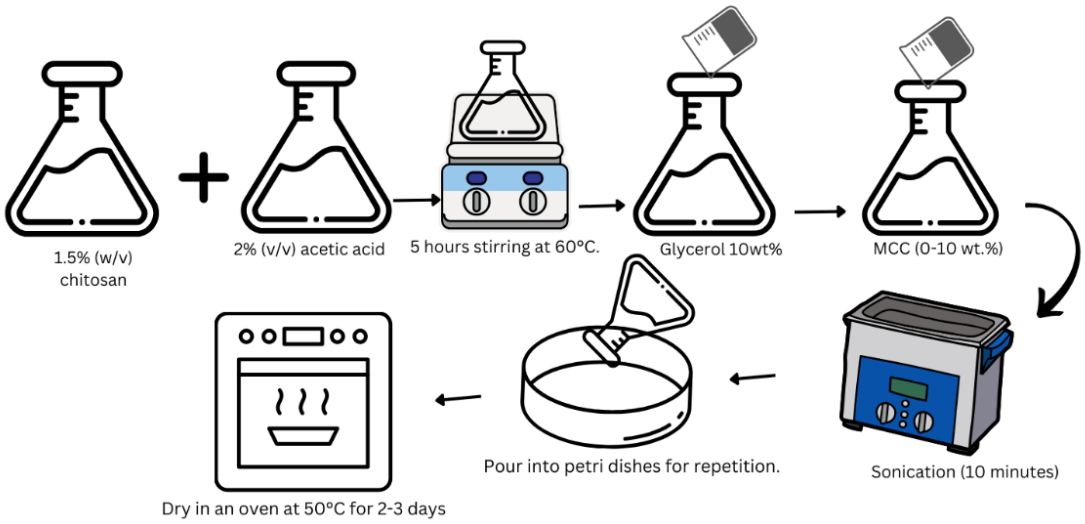

Figure 2: Systematic diagram of MCC/ MCH film preparation

2.8 Tensile Test

Tensile test was carried out using an Instron Universal Testing Machine at room temperature. (Instron 3366) and an ASTM method (ASTM D882) with a crosshead speed of 10 mm/min. The specimens were cut into rectangular strips with a length of 10 cm and width of 1 cm. The tensile strength, elongation at break, and Young's Modulus were measured. There are 5 samples that have been tested for each composition.

2.9 Fourier Transform Infrared Spectroscopy Analysis

Infrared spectra of pure mushroom chitosan and its composites were obtained in a range of 4000 cm^{-1} to 650 cm^{-1} wavenumber (16 scans) at a resolution of 4 cm^{-1} by using Perkin Elmer Spectrum 10 spectrophotometer. Attenuated total reflectance (ATR) technique was applied for this scanning method.

2.10 Scanning Electron Microscopy Analysis

The tensile fracture surface of MCC reinforced mushroom chitosan biocomposites was studied using scanning electron microscopy (SEM) (FEl Quanta 200F microscope). The films were examined with an accelerating voltage of 5 kV with a magnification of 500 x.

2.11 X-Ray Diffraction Analysis

With 30 mA of current at a voltage of 40 KV, X-ray diffraction (XRD) (Shidmazu 6000) was used to analyse the crystallinity of MCC reinforced chitosan biocomposites. The samples was scanned from 15° to 35° at a rate of 0.1 s/step and a speed of 2 °/min [17]. The crystallinity index (CI) was calculated using the Equation 1 [16].

$$CI(\%) = (I_{\_110} - I_{\_am})/I_{\_am} \times 100 \quad (1)$$

where $I_{\_110}$ was maximum intensity at 2θ and $I_{\_am}$ was intensity of amorphous diffraction at 2θ [18].

3. RESULTS AND DISCUSSION

3.1 Tensile Properties

Figure 3 shows the effect of different MCC content in the MCC/MCH biocomposites on tensile strength. Examining the influence of MCC loading on chitosan matrix revealed a notable pattern in tensile strength. At the 0 wt.% MCC content, the tensile strength of the MCC/MCH biocomposites stood at 26 MPa. The biocomposites showed the tensile strength with an increasing trend from 4 wt.% to 8 wt.% MCC content, reaching an optimal tensile strength of 33 MPa at 8% and reduced thereafter. MCC acts as a reinforcing filler in the chitosan matrix [19-20] The rise in tensile strength was attributed to the efficient transmission of stress through the percolating network created by the MCC within the chitosan matrix [21-22].

The favorable compatibility between the MCC filler and the chitosan matrix enhances a more uniform and efficient transfer of load between the chitosan and the MCC network. As a result, stress concentration in specific areas is effectively alleviated [23-24]. It is important to note that a 10% MCC loading resulted in a notable reduction in tensile strength, which measured 26 MPa. This might be the consequence of MCC's agglomeration and uneven distribution, which had the opposite effect on tensile strength [21].

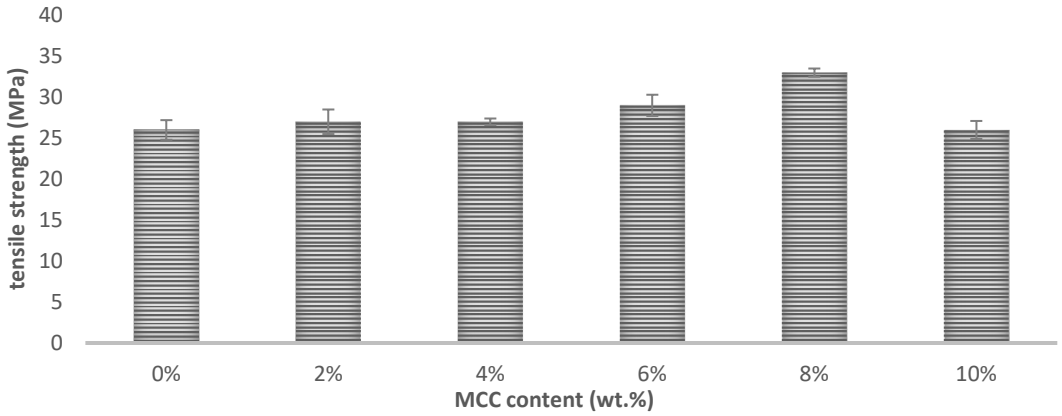

Figure 3: Tensile strength of MCC/MCH biocomposites with different MCC content

Figure 4 presents the elongation at break (EB) of MCC/MCH biocomposites with different MCC content. The EB characterizes the material's capacity to undergo changes in shape without experiencing the development of fractures. In contrast to the increase demonstrated by tensile strength, it was noticed that the incorporation of MCC reduced the elasticity of the films. Therefore, the ductility of the films will decrease with increasing concentrations of MCC. The EB reduced from 34% to 20% with the MCC loading ranging from 0% to 10%. These results are similar to the previous study of Pires et al. [25], providing justification for the reduction in EB due to the presence of cellulose materials, contributing to a dense layout with enhanced continuities within the polysaccharide network. The decrease in stretchability might be attributed to the development of inter-chain bonds, enhancing the cohesion within the polymer network but concurrently limiting the slippage of polymer chains during the pulling [26].

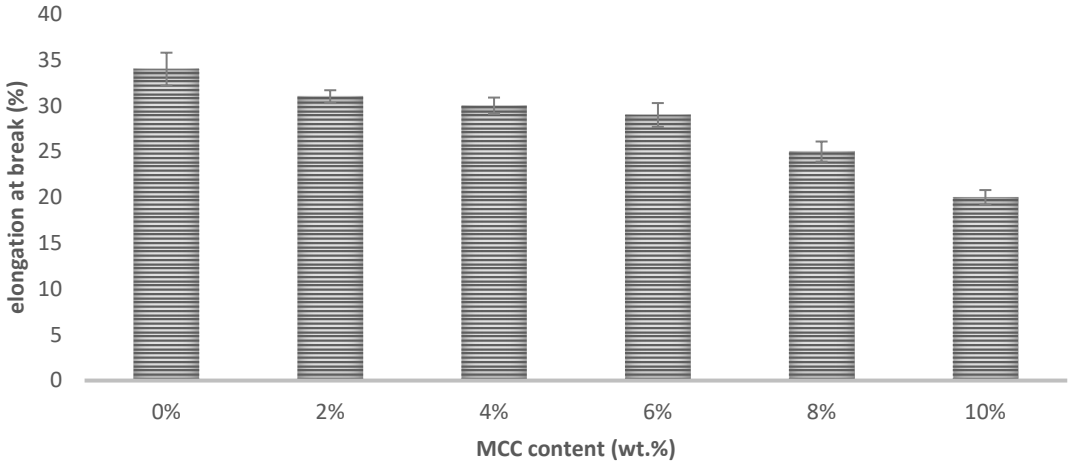

Figure 4: Elongation at break of MCC/MCH biocomposites with different MCC content

Figure 5 demonstrates the Young's modulus of MCC/MCH biocomposites with different MCC content**.** The Young's modulus of chitosan biocomposites exhibited the increasing trend. The elevated Young's modulus values can be attributed to the reinforcing influence caused by MCC in increased concentrations. This can be ascribed to the strong interaction of hydrogen bonds between MCC and chitosan molecules [27-28]. The MCC imparts added structural integrity to the composite material, leading to enhanced stiffness and improved mechanical properties, including a rise in Young's modulus [29]. As shown in Figure 7(d), the agglomeration also caused the reduction of tensile strength at 10% MCC content.

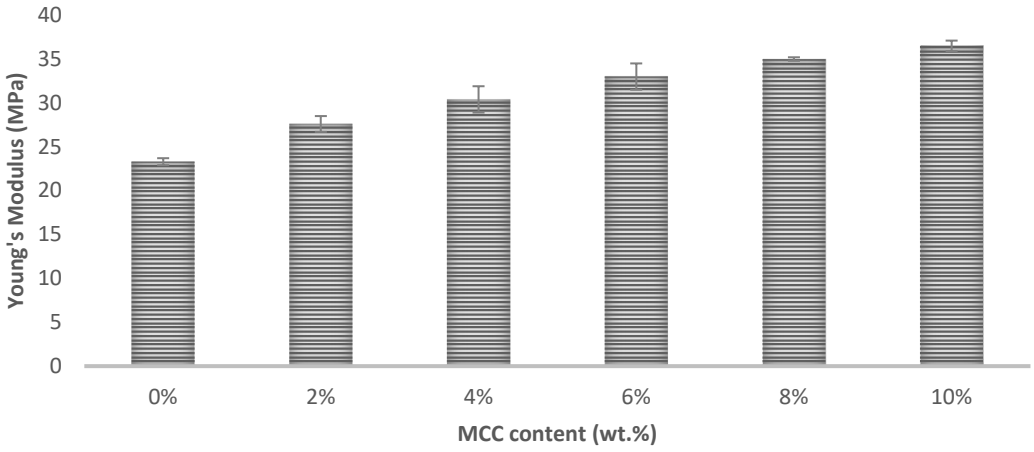

Figure 5: Young's modulus of MCC/MCH biocomposites with different MCC content

3.2 FTIR Analysis

Figure 6 displays the FTIR spectra of pure mushroom chitosan, 4% and 8% MCC/MCH biocomposites. The mushroom chitosan exhibited a broad transmission band at 3346 cm^{-1} for N-H and O-H stretching. The peak at 2930 cm^{-1} corresponds to CH_2 symmetric and asymmetric stretching, and these bands are typical polysaccharide

characteristics of chitosan[30]. For the MCC/MCH composites with 4% MCC and 8% MCC, the O-H intensity of the peak increased, indicating potential structural alterations or the presence of additional hydroxyl groups, possibly due to the interactions among MCC and chitosan, which may expose or generate new hydroxyl groups[31]. Furthermore, the peak ranging from 1600 cm^{-1} to 1700 cm^{-1} represents the C=O vibration from carboxylic acid, with its decreased intensity in 8% MCC/MCH biocomposites. The CH_2 bending and CH_3 symmetrical deformations were confirmed by the presence of bands at around 1420 cm^{-1}. The bands at 1040 cm^{-1} correspond to C-O stretching. All the bands appeared in the chitosan spectra reported by other researchers [30-32].

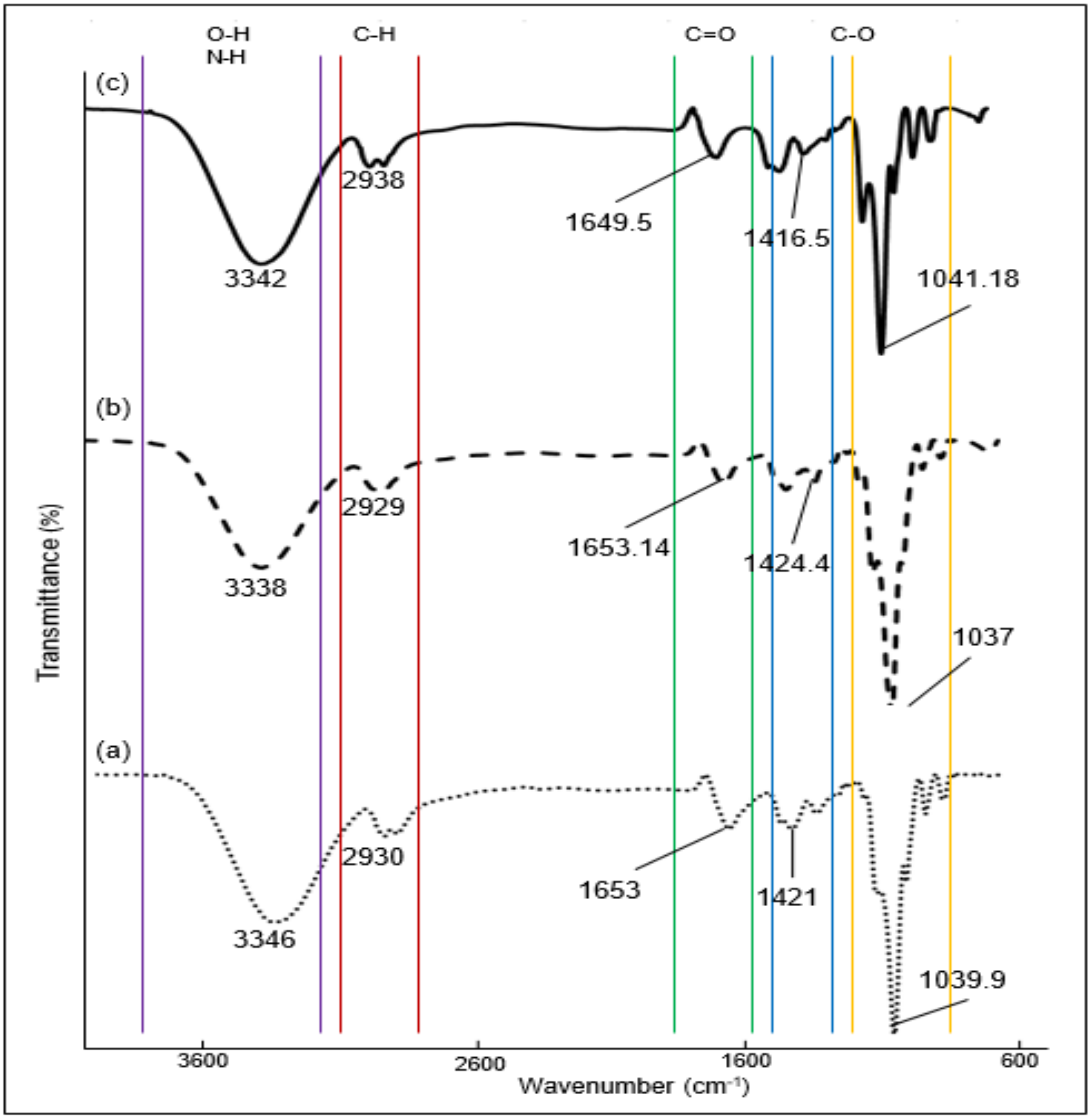

Figure 6: FTIR spectra of (a) pure mushroom chitosan, (b) 4% MCC and (c) 8% MCC biocomposites

3.3 SEM Analysis

Figure 7 shows the morphology of tensile fractured surface of MCC/MCH biocomposites with different MCC content. Figure 7(a) presented a smooth surface on the neat chitosan. Figure 7(b) displayed cleavage or transgranular fracture of the 4 wt% MCC. Increasing the MCC content had shown rougher surface and pores (Figure 7(c)-(d)) in which the elongation at break has been reduced gradually.

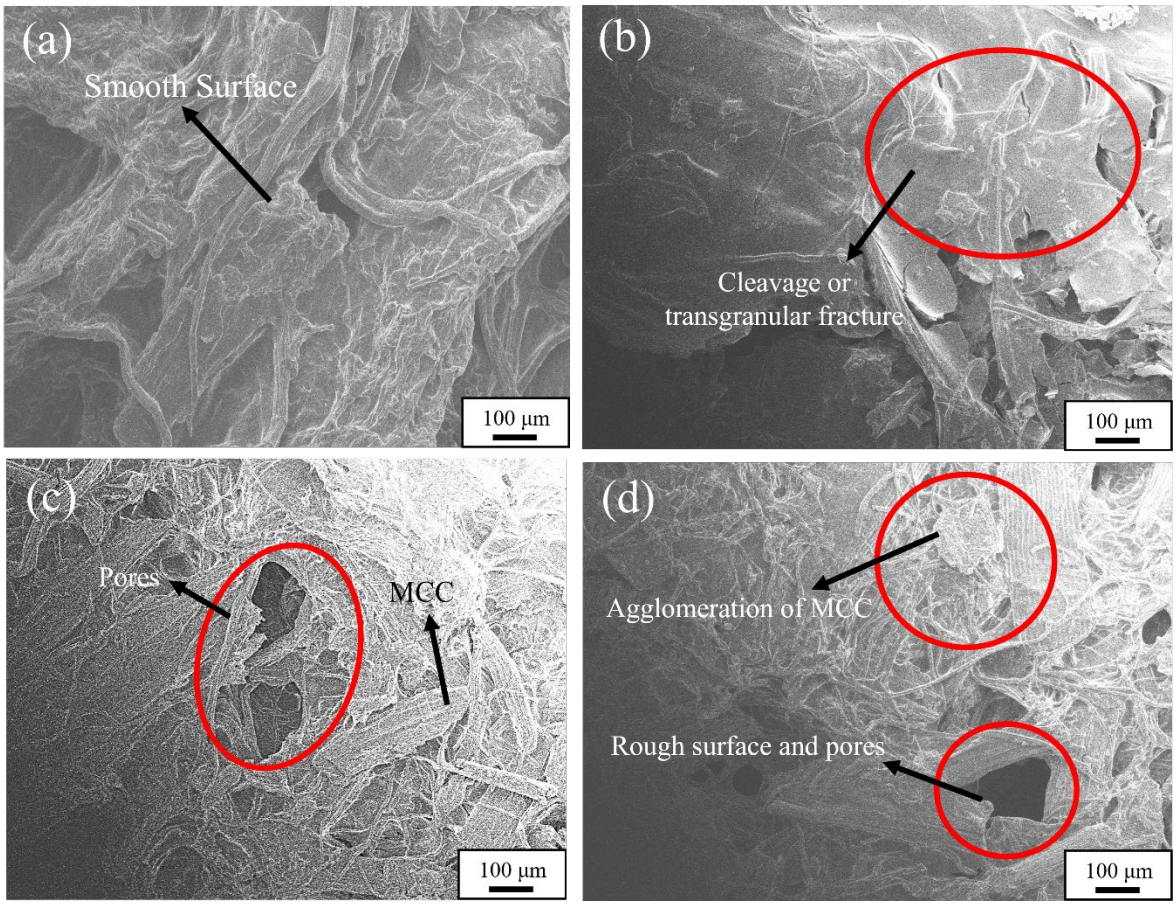

Figure 7: SEM micrographs of MCC/MCH biocomposites with (a) MCC 0%, (b) MCC 4%, (c) MCC 8% and (d) MCC 10%

3.4 XRD analysis

Figure 8 shows the XRD diffractogram of MCC powder, neat chitosan and MCC/MCH biocomposites. The pure MCC and all the MCH/MCC biocomposites indicated the maximum peak at around $2\theta = 23^{o}$ in XRD diffractogram, however the peak at $2\theta = 23^{o}$ was lower in MCH/MCC biocomposites. The crystallinity index of MCC powder decreased when it was added into chitosan. This outcome indicated that the incorporation of MCC into chitosan biocomposites has the potential to disrupt or alter the crystal structure of MCC. The mixing and processing stages involved in the preparation of MCC/MCH biocomposites may introduce mechanical forces or other factors that destabilize the crystalline regions of MCC, resulting in a lower crystallinity index [33].

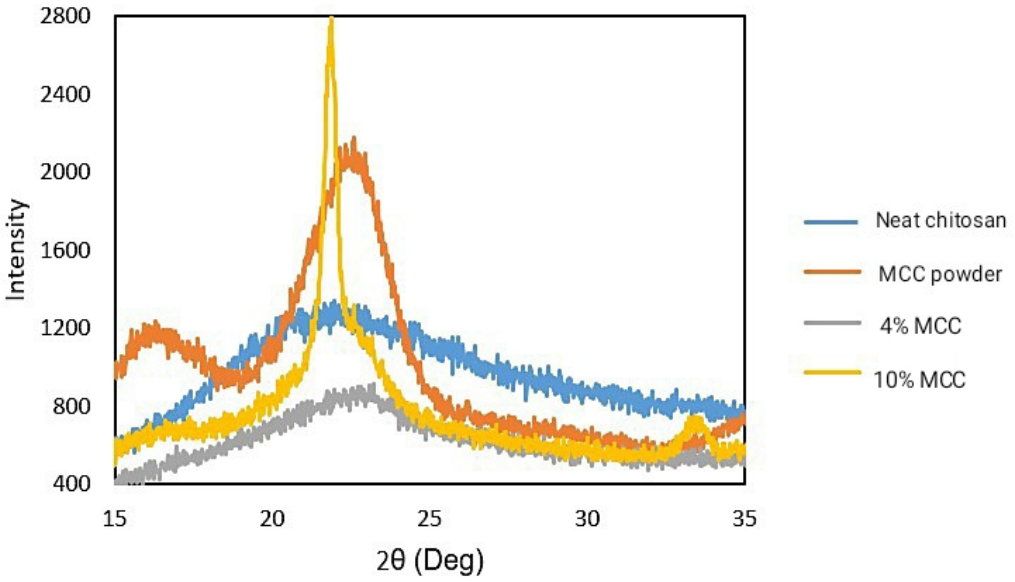

Figure 8. XRD diffractogram of neat chitosan, MCC powder and MCC/MCH biocomposites

An increment of crystallinity index of MCC/MCH biocomposites with difference content of MCC is summarized in Table 1. According to Bhasney et al. [34]. the addition of the MCC content in chitosan biocomposites can induce the crystallinity increment. This is possible if the added MCC functions as a nucleating agent and promotes the formation of additional crystalline regions within the biocomposites. The presence of MCC can improve the alignment and packaging of cellulose chains, resulting in a greater crystallinity than the neat chitosan matrix alone.

Table 1: Crystallinity percentage of MCC powder and different MCC content in MCC/MCH biocomposites

Sample	Crystallinity Index (%)
MCC	71.5
Neat chitosan	43.4
MCC 4% / chitosan	54.5
MCC 10% / chitosan	62.3

4. CONCLUSIONS

In conclusion, the biocomposite films of MCC/MCH exhibited optimal tensile strength at 8 wt%. Nevertheless, elongation at break demonstrated reduction with the addition of MCC whereas Young's modulus presented increment trend. SEM analysis indicated that the biocomposites with lower MCC loading had fewer pores on the surface compared to those with higher MCC content. XRD analysis showed that all the MCH/MCC biocomposites and pure MCC displayed a maximum peak at around $2\theta = 23^{o}$, but the peak intensity at this angle was lower in the MCH/MCC biocomposites. The findings suggest that the 8 wt% MCC in the MCC/MCH biocomposite films offers a favorable balance of tensile strength, highlighting the potential for further applications in packaging or related industries.

Acknowledgements

The authors wish to thank to the research funding namely Fundamental Research Grant Scheme (FRGS/1/2022/TK09/UNIMAP/02/21) from Ministry of Higher Education Malaysia.

Author Contributions

All authors contributed toward data analysis, drafting and critically revising the paper and agree to be accountable for all aspects of the work.

Disclosure of Conflict of Interest

The authors declare no potential conflict of interest in the publication of this work.

Compliance with Ethical Standards

The work is compliant with ethical standards.

References

[1] Cao, L., Liu, W., & Wang, L. (2018). Developing a green and edible film from Cassia gum: The effects of glycerol and sorbitol. *Journal of Cleaner Production*; *175*, 276–282.

[2] Hassan, B., Chatha, S. A. S., Hussain, A. I., Zia, K. M., & Akhtar, N. (2018). Recent advances on polysaccharides, lipids and protein based edible films and coatings: A review. *International Journal of Biological Macromolecules*, *109*, 1095–1107.

[3] Sun, L., Sun, J., Chen, L., Niu, P., Yang, X., & Guo, Y. (2017). Preparation and characterization of chitosan film incorporated with thinned young apple polyphenols as an active packaging material. *Carbohydrate Polymers*, *163*, 81–91.

[4] Khalil, H. P. S. A., Tye, Y. Y., Saurabh, C. K., Leh, C. P., Lai, T. K., Chong, E. W. N., Fazita, M. R. N., Hafiidz, J. M., Banerjee, A., & Syakir, M. I. (2017). Biodegradable polymer films from seaweed polysaccharides: A review on cellulose as a reinforcement material. *Express Polymer Letters*, *4*, 244–265.

[5] Sathiyabama, M., Akila, G., & Charles, R. E. (2014). Chitosan-induced defence responses in tomato plants against early blight disease caused by alternaria solani (Ellis and Martin) Sorauer. *Archives of Phytopathology and Plant Protection*, *47*, 1963–1973.

[6] Islam, M. M., Shahruzzaman, M., Biswas, S., Sakib, M. N., & Rashid, T. U. (2020). Chitosan based bioactive materials in tissue engineering applications-A review. *Bioactive Materials*, *5*, 164–183.

[7] Huq, T., Khan, A., Brown, D., Dhayagude, N., He, Z., & Ni, Y. (2022). Sources, production and commercial applications of fungal chitosan: A review. *Journal of Bioresources and Bioproducts, 7*, 85–98.

[8] Dentinger, B. T., Ammirati, J. F., Both, E. E., Desjardin, D. E., Halling, R. E., Henkel, T. W., Moreau, P., Nagasawa, E., Soytong, K., Taylor, A. F., Watling, R., Moncalvo, J., & McLaughlin, D. J. (2010). Molecular phylogenetics of porcini mushrooms (Boletus section Boletus). *Molecular Phylogenetics and Evolution*, *57*,1276–1292.

[9] Cui, Y., Feng, B., Wu, G., Xu, J., & Yang, Z. L. (2015). Porcini mushrooms (Boletus sect. Boletus) from China. *Fungal Divers*, 81, 189–212.

[10] Bessette, A. E., Roody, W. C., & Bessette, A. R. (2017). *Boletes of Eastern North America*. (Syracuse: Syracuse University Press.) pp. 245-247

[11] Mat Zin, M. I., Jimat, D. N., & Wan Nawawi, W. M. F. (2022). Physicochemical properties of fungal chitin nanopaper from shiitake (L. edodes), enoki (F. velutipes) and oyster mushrooms (P. ostreatus). *Carbohydrate Polymers*, *281*.

[12] Botta, L., Titone, V., Mistretta, M. C., La Mantia, F. P., Modica, A., Bruno, M., Sottile, F., & Lopresti, F. (2021). PBAT based composites reinforced with microcrystalline cellulose obtained from softwood almond shells. *Polymers (Basel)*, *13*.

[13] Ratnakumar, A., Rathnayake, W. S. M., Karunanayake, L., Samarasekara, A. M. P. B., & Amarasinghe, D.A.S. (2020). Microcrystalline cellulose as reinforcing agents for polypropylene composites. *Tropical Agricultural Research*, 31, 106.

[14 Bangar, S. P., Esua, O. J., Nickhil, C., & Whiteside, W. S. (2023). Microcrystalline cellulose for active food packaging applications: A review. *Food Packaging and Shelf Life*, *36*.

[15] Johney, J., Eagappan, K., & Ragunathan, R. R. (2016). Microbial extraction of chitin and chitosan from Pleurotus spp, its characterization and antimicrobial activity. *International Journal of Current Pharmaceutical Research,* 9, 88.

[16] Gan, P. G., Sam, S. T., Abdullah, M., Omar, M. F., & Tan, W. K. (2021). Water resistance and biodegradation properties of conventionally-heated and microwave-cured cross-linked cellulose nanocrystal/chitosan composite films. *Polymer Degradation and Stability, 188*, 109563.

[17] Converse, E. S., Thorpe, F., Rivera, J., Charalambous, H., King, G., Cahill, J. T., Du Frane, W. L., Kuntz, J. D., & McCormack, S. J. (2023). In-situ synchrotron x-ray diffraction and thermal expansion of TiB2 up to ∼3050 °C. *Journal of the European Ceramic Society*, *43*, 3005–3012.

[18] Kamaludin, N. H. I., Ismail, H., Rusli, A., & Ting, S. S. (2020). Thermal behavior and water absorption kinetics of polylactic acid/chitosan biocomposites. *Iranian Polymer Journal*, *30*, 135–147.

[19] Banerjee, G., & Ray, A. K. (2017). Impact of microbial proteases on biotechnological industries. *Biotechnology and Genetic Engineering Reviews*, *33*, 119–143.

[20] Aguilar, J. G. D. S., & Sato, H. H. (2018). Microbial proteases: Production and application in obtaining protein hydrolysates. *Food Research International*, *103*, 253–262.

[21] Gan, P. G., Sam, S. T., Abdullah, M. F., Omar, M. F., & Tan, W. K. (2020). Comparative study on the properties of cross-linked cellulose nanocrystals/chitosan film composites with conventional heating and microwave curing. *Journal of Applied Polymer Science*, *137*.

[22] Suklaw, N., & Ratanakamnuan, U. (2022). Mechanical properties and biodegradability of starch-based biocomposite films reinforced with microcrystalline cellulose from rice embryo. *Journal of Physics. Conference Series, 2175.* 012034.

[23] Debnath, B., Duarah, P., Haldar, D., & Purkait, M. K. (2022). Improving the properties of corn starch films for application as packaging material via reinforcement with microcrystalline cellulose synthesized from elephant grass. *Food Packaging Shelf Life*, *34*, 100937.

[24] Khan, A., Khan, R. A., Salmieri, S., Tien, C. L., Riedl, B., Bouchard, J., Chauve, G., Tan, V., Kamal, M. R., & Lacroix, M. (2012). Mechanical and barrier properties of nanocrystalline cellulose reinforced chitosan based nanocomposite films. *Carbohydrate Polymers*, *90*, 1601–1608.

[25] Pires, J. R., Souza, V. G., Gomes, L. A., Coelhoso, I. M., Godinho, M. H., & Fernando, A. L. (2022). Micro and nanocellulose extracted from energy crops as reinforcement agents in chitosan films. *Industrial Crops and Products*, *186,* 115247.

[26] Perumal, A. B., Sellamuthu, P. S., Nambiar, R. B., & Sadiku, E. R. (2018). Development of polyvinyl alcohol/chitosan bio-nanocomposite films reinforced with cellulose nanocrystals isolated from rice straw. *Applied Surface Science*, *449*, 591–602.

[27] De Souza Coelho, C. C., Silva, R. B. S., Carvalho, C. W. P., Rossi, A. L., Teixeira, J. A., Freitas-Silva, O., & Cabral, L. M. C. (2020). Cellulose nanocrystals from grape pomace and their use for the development of starch-based nanocomposite films. *International Journal of Biological Macromolecules*, *59,* 1048–1061.

[28] Kumar, A., Negi, Y. S., Choudhary, V., & Bhardwaj, N. K. (2014). Effect of modified cellulose nanocrystals on microstructural and mechanical properties of polyvinyl alcohol/ovalbumin biocomposite scaffolds. *Materials Letters*, *129*, 61–64.

[29] Nuradibah, M., Yusoff, N., Sam, S., & Jejawi, P. (2018). effect of adipic acid as crosslinking agent in polyvinyl alcohol / nanocellulose from rice straw biocomposites. *Journal of Engineering Research and Education, 10,* 79-84.

[30] Chen, Y., Nie, Z., Gao, J., Wang, J., & Cai, M. (2021). A novel adsorbent of bentonite modified chitosan-microcrystalline cellulose aerogel prepared by bidirectional regeneration strategy for Pb(II) removal. *Journal of Environmental Chemical Engineering*, *9*, 105755.

[31] Beji, E., Keshk, S. M., Douiri, S., Charradi, K., Hassen, R. B., Gtari, M., Attia, H., & Ghorbel, D. (2023). Bioactive film based on chitosan incorporated with cellulose and aluminum chloride for food packaging application: Fabrication and characterization. *Food Bioscience*, *53*, 102678.

[32] Bhat, A. H., Khan, I., Usmani, M. A., Umapathi, R., & Al-Kindy, S. M. Z. (2019). Cellulose an ageless renewable green nanomaterial for medical applications: An overview of ionic liquids in extraction, separation and dissolution of cellulose. *International Journal of Biological Macromolecules*, *129*, 750–777

[33] Izzati, A. N. A., John, W. C., Fazita, M. R. N., Najieha, N., Azniwati, A. A., & Khalil, H. P. S. A. (2020). Effect of empty fruit bunches microcrystalline cellulose (MCC) on the thermal, mechanical and morphological properties of biodegradable poly (lactic acid) (PLA) and polybutylene adipate terephthalate (PBAT) composites. *Materials Research Express*, *7*, 015336.

[34] Bhasney, S. M., Kumar, A., & Katiyar, V. (2020). Microcrystalline cellulose, polylactic acid and polypropylene biocomposites and its morphological, mechanical, thermal and rheological properties. *Composites Part B: Engineering*, *184*, 107717.